Entanglement Swapping between Discrete and Continuous Variables

Shuntaro Takeda,[1] Maria Fuwa,[1] Peter van Loock,[2] and Akira Furusawa[1,*]
[1]Department of Applied Physics, School of Engineering, The University of Tokyo, 7-3-1 Hongo, Bunkyo-ku, Tokyo 113-8656, Japan
[2]Institute of Physics, Johannes Gutenberg-Universität Mainz, Staudingerweg 7, 55128 Mainz, Germany
(Received 5 November 2014; revised manuscript received 2 February 2015; published 9 March 2015)

We experimentally realize "hybrid" entanglement swapping between discrete-variable (DV) and continuous-variable (CV) optical systems. DV two-mode entanglement as obtainable from a single photon split at a beam splitter is robustly transferred by means of efficient CV entanglement and operations, using sources of squeezed light and homodyne detections. The DV entanglement after the swapping is verified without postselection by the logarithmic negativity of up to 0.28 ± 0.01. Furthermore, our analysis shows that the optimally transferred state can be postselected into a highly entangled state that violates a Clauser-Horne-Shimony-Holt inequality by more than 4 standard deviations, and thus it may serve as a resource for quantum teleportation and quantum cryptography.

DOI: 10.1103/PhysRevLett.114.100501 PACS numbers: 03.67.Bg, 03.65.Ud, 03.67.Hk, 42.50.Ex

Quantum entanglement can be created between two distant quantum systems that have never directly interacted. This effect, called entanglement swapping [1–8], is a building block for quantum communication and computation [9–12]. It was originally proposed and demonstrated for discrete-variable (DV) optical systems [1–4]. The protocol starts with two entangled pairs, A-B and C-D, each represented either by twin photons or by a single photon split into two distinct modes [Fig. 1(a)]. A joint projective measurement of B and C onto one of the four two-qubit Bell states then leads to an entangled state for A and D, even though A and D never directly interact with each other. Entanglement swapping can also be interpreted as the transfer of one half of an entangled state, either from B to D or from C to A, by quantum teleportation [13]. It is a key element for quantum networking [9], quantum computing [10], quantum cryptography [14], and especially long-distance quantum communication by means of quantum repeaters [11,12]. However, in this DV setting solely based upon single photons, due to the heralded conditional entangled-state generation and the probabilistic linear-optics Bell-state measurement (BSM), successful entanglement swapping events occur very rarely. As a result, in a quantum repeater, for example, long-distance entangled-pair creation rates would be correspondingly low and requirements on the coherence times of the local quantum memories at each repeater station impractically high. In addition, the observation and verification of the final entanglement between A and D in the DV scheme typically requires postselection.

Entanglement swapping was later extended to continuous-variable (CV) systems [15,16], where the pairs A-B and C-D each correspond to the two modes of a two-mode squeezed, quadrature-entangled state [5,6] [Fig. 1(b)]. Since such entangled states are available on demand and a linear-optics BSM in the quadrature basis can be performed without failure, entanglement can be swapped deterministically and verified without postselection [7,8]. However, due to the finite squeezing of both initial entanglement sources, the final entanglement after swapping in the CV scheme is inevitably degraded by excess noise. In fact, the entanglement drops exponentially [17,18], and in practice, CV entanglement swapping can always be replaced by a direct transmission through a lossy channel [19]. Moreover, purification techniques for this type of degraded entanglement are not so advanced at present [20,21].

Our scheme combines the best features of the above two approaches, making use of both DV and CV entanglement

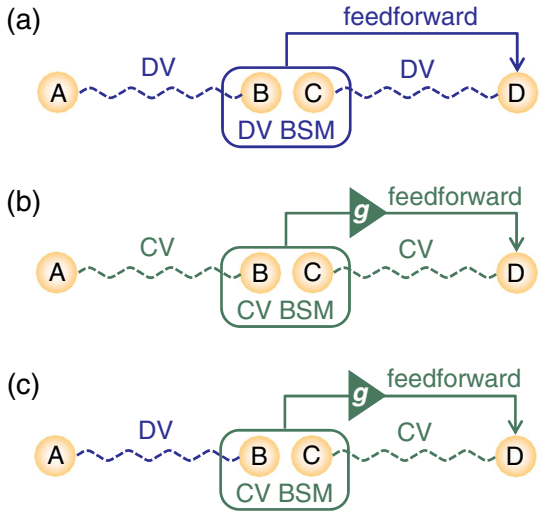

FIG. 1 (color online). Schematic of entanglement swapping. (a) DV entanglement swapping, (b) CV entanglement swapping, (c) hybrid entanglement swapping.

at the same time [Fig. 1(c)]. By means of CV teleportation [22,23], using squeezed-state entanglement, homodyne-based BSM, and feedforward by phase-space displacement, DV entanglement is transferred from A-B to A-D. Once the initial single-photon entanglement is conditionally prepared in modes A and B, all the remaining steps of our scheme are unconditional, achieving a highly efficient transfer of the DV entanglement. Because optical CV quantum teleportation runs in a deterministic fashion (as opposed to optical DV quantum teleportation) and DV entanglement is robust against loss (as opposed to CV entanglement), entanglement is efficiently and reliably transferred only in this "hybrid" setting. Furthermore, as will be explained below, a maximally entangled state can be obtained after the swapping through postselection, even though only finitely squeezed resources are used.

In this hybrid setting, the DV entanglement can be transferred for any nonzero squeezing, as is theoretically shown in Refs. [24,25]. Our setup (Fig. 2) uses the DV entanglement in the form of a photon split at a beam splitter with reflectivity R, described by $|\psi\rangle_{AB} = \sqrt{1-R}|1\rangle_A|0\rangle_B + \sqrt{R}|0\rangle_A|1\rangle_B$ in the two-mode photon number basis. This state is maximally entangled when $R = 0.5$. In contrast, the CV entanglement is a two-mode squeezed state, $\sqrt{1-g_{\rm opt}}\sum_{n=0}^{\infty} g_{\rm opt}^n|n\rangle_C|n\rangle_D$, with $g_{\rm opt} \equiv \tanh r$, where r is the squeezing parameter. Though this state is nonmaximally entangled for finite r, the DV entanglement can be transferred for any $r > 0$ by tuning the feedforward gain to $g_{\rm opt}$, when the final state of D is an imperfect version of the initial state of B attenuated by a factor $1 - g_{\rm opt}^2$ [24,25]. At this gain, the initial entangled state at $R = 0.5$ is swapped and transformed according to

$$\hat{\rho}_{AB} \equiv |\psi\rangle_{AB}\langle\psi| \rightarrow \hat{\rho}_{AD} \equiv \frac{1+g_{\rm opt}^2}{2}|\psi'\rangle_{AD}\langle\psi'| + \frac{1-g_{\rm opt}^2}{2}|0,0\rangle_{AD}\langle 0,0|, \quad (1)$$

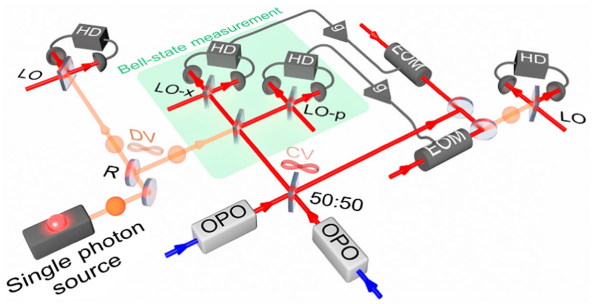

FIG. 2 (color online). Experimental layout. DV entanglement is created by splitting a heralded single photon [29], while CV entanglement is created on demand by mixing two squeezed beams from optical parametric oscillators (OPOs). The state after entanglement swapping is characterized by homodyne tomography [30,31]. EOM, electro-optic modulator; HD, homodyne detector; LO, local oscillator.

where $|\psi'\rangle_{AD} = (|1\rangle_A|0\rangle_D + g_{\rm opt}|0\rangle_A|1\rangle_D)/(1+g_{\rm opt}^2)^{1/2}$. Here, the initial maximally entangled state $|\psi\rangle_{AB}$ is converted into a nonmaximally entangled state $|\psi'\rangle_{AD}$ mixed with an extra two-mode vacuum term. When $g_{\rm opt} > 0$, $\hat{\rho}_{AD}$ violates the positivity after partial transposition; this shows that DV entanglement remains present after teleportation for any $r > 0$ by optimal gain tuning [26]. Since no additional photons are created in $\hat{\rho}_{AD}$, it can be used for teleportation [27], swapping [3], and purification protocols [28].

The present experimental setup (Fig. 2) is an extended version of the setup in Ref. [23]. We use a continuous-wave Ti:sapphire laser at 860 nm. A heralded single photon with a HWHM of 6.2 MHz is created from a nondegenerate optical parametric oscillator (OPO) at a rate of 7000 s^{-1} [29]. The photon when incident on a beam splitter of reflectivity $R = 0.50$ or $R = 0.67$ yields a DV entangled state $|\psi\rangle_{AB}$. The CV entangled state is deterministically generated by combining at a beam splitter two squeezed vacua each produced from a degenerate OPO with a HWHM of 12 MHz. A CV BSM is performed jointly on the two corresponding halves of these two entangled states by combining them at a 50:50 beam splitter and then measuring the orthogonal quadratures of the output modes by homodyne detection. The homodyne signals are multiplied by a factor g and used for modulating auxiliary coherent beams. These beams are combined with the other half of the CV entangled state, thereby displacing the state in phase space. Tomographic reconstruction of the initial and final states, $\hat{\rho}_{AB}$ and $\hat{\rho}_{AD}$, are performed by two homodyne measurements with local oscillators' phases θ_1 and θ_2. For these particular states, the sum $\theta_1 + \theta_2$ does not affect the homodyne statistics in theory [25]. Thus, we first confirm the sum independence of the homodyne statistics and then scan only the relative phase $\theta_1 - \theta_2$ for tomography [30]. For every state, 100 000 sets of quadrature and phase values are acquired and used for a maximum likelihood algorithm without compensation of the measurement inefficiency [31].

The experimental density matrix of the initial DV entangled state $\hat{\rho}_{AB}$ at $R = 0.5$ is shown in Fig. 3(a). This state includes $80.6 \pm 0.3\%$ of the ideal $|\psi\rangle_{AB}$, $18.3 \pm 0.3\%$ of vacuum, and $1.1 \pm 0.2\%$ of multiphoton terms. The density matrices of the swapped states, $\hat{\rho}_{AD}$, at $r = 0.71$, $g = 0.63$ ($g_{\rm opt} = 0.61$) and $r = 1.01$, $g = 0.79$ ($g_{\rm opt} = 0.77$) are also shown in Figs. 3(b) and 3(c), respectively [32]. It can be seen that only one mode of the entangled state is attenuated by a factor close to $1 - g_{\rm opt}^2$, but the off-diagonal elements ($|0,1\rangle\langle 1,0|$ and $|1,0\rangle\langle 0,1|$) are still preserved, indicating that the DV entanglement remains present after the swapping. The amount of entanglement can be assessed by the logarithmic negativity, $E(\hat{\rho}) \equiv \log_2\|\hat{\rho}^{\Gamma}\|$, where $\|\hat{\rho}\| \equiv {\rm Tr}(\hat{\rho}^{\dagger}\hat{\rho})^{1/2}$ is the trace norm and Γ denotes partial transposition with regards to one of the subsystems [33–35]. The gain dependence of $E(\hat{\rho}_{AD})$ at $r = 0$, $r = 0.71$, and $r = 1.01$ is plotted in Fig. 3(d). Though the values of $E(\hat{\rho}_{AD})$

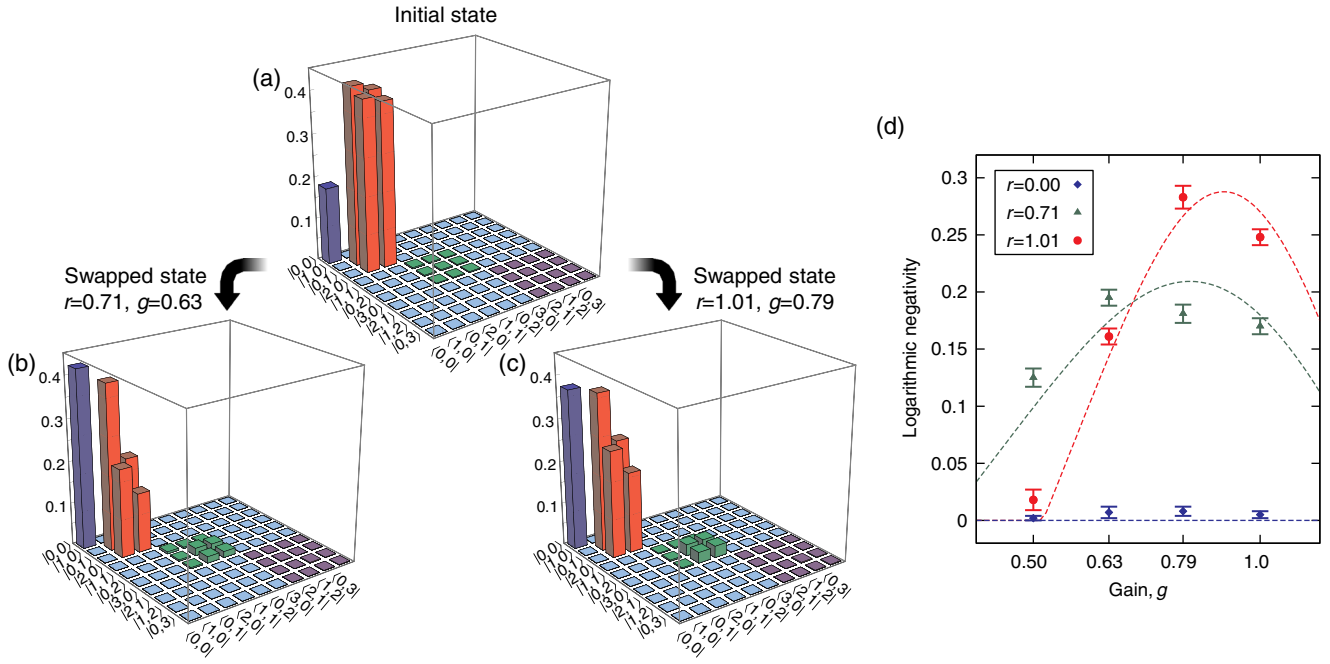

FIG. 3 (color online). Experimental results. (a)–(c) Density matrices of $\hat{\rho}_{AB}$ (a), $\hat{\rho}_{AD}$ at $r = 0.71$ and $g = 0.63$ (b), and $\hat{\rho}_{AD}$ at $r = 1.01$ and $g = 0.79$ (c). The absolute value of each matrix element is plotted. (d) Gain dependence of the logarithmic negativity for $r = 0$ (blue diamonds), $r = 0.71$ (green triangles), and $r = 1.01$ (red circles). Theoretical curves are also plotted in the same colors.

are reduced from the initial value of $E(\hat{\rho}_{AB}) = 0.71 \pm 0.01$, the positive values of $E(\hat{\rho}_{AD})$ at $r > 0$ clearly demonstrate the successful entanglement swapping. As expected, no entanglement is observed for $r = 0$. These results also confirm the quantum nature of CV quantum teleportation [22] in transferring DV systems [23]. The transferred entanglement from A-B to A-D [$E(\hat{\rho}_{AD}) = 0.28 \pm 0.01$ at the maximum] is much greater than in the previous swapping experiments for discrete variables [2–4], which postselectively transferred the initial entanglement with a probability less than 1%, corresponding to $E(\hat{\rho}_{AD}) < 0.01$ without postselection. We also performed the experiment for $R = 0.67$ and observed $E(\hat{\rho}_{AD}) > 0$ for $r = 0.71$ and $r = 1.01$ [36].

The final state, $\hat{\rho}_{AD}$, is contaminated with an extra vacuum due to the finite squeezing r; however, it can be, in principle, purified to a maximally entangled state postselectively [12]. Remarkably, this also works for any $r > 0$, even though the pure-state component in $\hat{\rho}_{AD}$ is itself only a nonmaximally entangled state for finite squeezing (as opposed to the maximally entangled Bell-state fractions in the scheme of Ref. [12]). The purification is achieved by first preparing two copies of $\hat{\rho}_{AD}$, written as $\hat{\rho}_{A_1D_1} \otimes \hat{\rho}_{A_2D_2}$, and then projecting this state onto the subspace with one photon in each location, corresponding to $\{|1\rangle_{A_1}|0\rangle_{A_2}, |0\rangle_{A_1}|1\rangle_{A_2}\} \otimes \{|1\rangle_{D_1}|0\rangle_{D_2}, |0\rangle_{D_1}|1\rangle_{D_2}\} \equiv \{|A_1\rangle, |A_2\rangle\} \otimes \{|D_1\rangle, |D_2\rangle\}$. When $\hat{\rho}_{AD}$ has the form of Eq. (1), this projection leads to a maximally entangled state, $(|A_1\rangle|D_2\rangle + |A_2\rangle|D_1\rangle)/\sqrt{2}$, regardless of the squeezing level $r > 0$. In other words, in principle, the hybrid setting allows for transferring maximally entangled states by means of finitely squeezed resources with a finite success probability, which in our experiment is already an order of magnitude larger compared to Refs. [2–4] (see below) and can be further increased for higher squeezing.

We perform this purification protocol by analytically extracting the corresponding subspace from two copies of the experimental $\hat{\rho}_{AD}$ [36]. The renormalized density matrices after postselection $\hat{\rho}_{AD}^{\mathrm{ps}}$, calculated from $\hat{\rho}_{AD}$ in Figs. 3(b) and 3(c), are shown in Figs. 4(a) and 4(b), respectively. The probability for the state being projected onto $\hat{\rho}_{AD}^{\mathrm{ps}}$ is $12.5 \pm 0.2\%$ and $16.0 \pm 0.3\%$, respectively, which is calculated as the trace of the postselected subspace. It can be seen that both states are almost purified to the maximally entangled state $(|A_1\rangle|D_2\rangle + |A_2\rangle|D_1\rangle)/\sqrt{2}$. For the ideal $\hat{\rho}_{AD}$ in Eq. (1), the $|A_1D_1\rangle\langle A_1D_1|$ and $|A_2D_2\rangle\langle A_2D_2|$ elements should be zero after postselection. The small contributions of these terms in Figs. 4(a) and 4(b) originate from the multiphoton term $|1,1\rangle\langle 1,1|$ in $\hat{\rho}_{AD}$, and this term is mainly attributed to the impurity of squeezing. The values of the logarithmic negativity, $E(\hat{\rho}_{AD}^{\mathrm{ps}}) = 0.67 \pm 0.02$ for Fig. 4(a) and $E(\hat{\rho}_{AD}^{\mathrm{ps}}) = 0.75 \pm 0.02$ for Fig. 4(b), are greater than those without postselection, demonstrating the purification of the entanglement. In addition, the postselected state can be used for measuring violations of Bell's inequality by the setup shown in Fig. 4(c) [12]. Our calculation shows that the postselected state in Figs. 4(a) and 4(b) can, in principle, violate the Clauser-Horne-Shimony-Holt inequality [37]

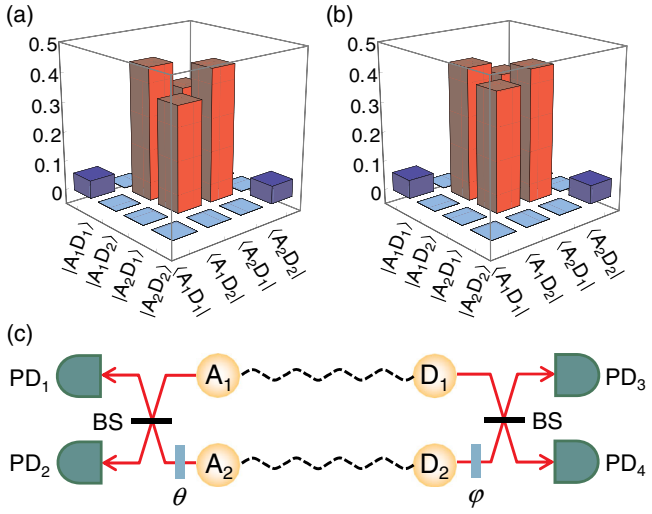

FIG. 4 (color online). Analysis with postselection. (a) $\hat{\rho}_{AD}^{\mathrm{ps}}$ calculated from $\hat{\rho}_{AD}$ at $r = 0.71$ and $g = 0.63$ [Fig. 3(b)]. (b) $\hat{\rho}_{AD}^{\mathrm{ps}}$ calculated from $\hat{\rho}_{AD}$ at $r = 1.01$ and $g = 0.79$ [Fig. 3(c)]. (c) Schematic setup for the realization of Bell's inequality detection with postselection. The values of the S parameter estimated in the main text correspond to those values that would be measured in this setup. The setup consists of two entangled pairs (A_1-D_1, A_2-D_2), phase shifters (θ, ϕ), 50:50 beam splitters (BS), and photon detections (PD_1–PD_4).

by the estimated S parameters of $S = 2.08 \pm 0.05 > 2$ and $S = 2.21 \pm 0.05 > 2$, respectively (the latter indicates the violation by more than 4 standard deviations). These highly entangled states can be directly used for quantum key distribution with the same setup as in Fig. 4(c) [12]. These states would also enable one to do quantum teleportation of qubits [36], and the estimated fidelities of 0.86 ± 0.01 and 0.89 ± 0.01 are well beyond the classical limit [38] of $2/3$.

In conclusion, we demonstrated a "hybrid" entanglement swapping scheme, transferring robust DV entanglement in the form of a split photon by means of efficient CV entanglement and operations. By tuning the feedforward gain of the teleporter, entanglement is reliably and efficiently transferred, and then verified unconditionally. Moreover, despite the finite squeezing of the CV entanglement resource, the DV states after the swapping can always be postselected into highly entangled states that violate Bell's inequality and may serve as resources for advanced quantum information protocols. These results imply many possibilities for near-future applications of hybrid quantum networks, where more general forms of DV entanglement may be efficiently transferred or manipulated with the help of CV techniques. In a realistic network, where both the DV and the CV parts would be subject to transmission losses during their distributions, it is then better to have the loss-sensitive CV links shorter than the loss-robust DV links or, in the most extreme scenario, to employ the CV entanglement only as a local on-demand resource, for instance, in order to deterministically load some local quantum memories [39].

This work was partially supported by the SCOPE program of the MIC of Japan, PDIS, GIA, and APSA commissioned by the MEXT of Japan, FIRST initiated by CSTP, and ASCR-JSPS. S. T. and M. F. acknowledge financial support from ALPS. P. v. L. was supported by QcomQ (BMBF) and HIPERCOM (ERA-Net CHIST-ERA). We thank Masato Koashi for useful discussions.

*akiraf@ap.t.u-tokyo.ac.jp

[1] M. Żukowski, A. Zeilinger, M. A. Horne, and A. K. Ekert, Phys. Rev. Lett. **71**, 4287 (1993).
[2] J.-W. Pan, D. Bouwmeester, H. Weinfurter, and A. Zeilinger, Phys. Rev. Lett. **80**, 3891 (1998).
[3] F. Sciarrino, E. Lombardi, G. Milani, and F. De Martini, Phys. Rev. A **66**, 024309 (2002).
[4] H. de Riedmatten, I. Marcikic, J. A. W. van Houwelingen, W. Tittel, H. Zbinden, and N. Gisin, Phys. Rev. A **71**, 050302(R) (2005).
[5] S. M. Tan, Phys. Rev. A **60**, 2752 (1999).
[6] P. van Loock and S. L. Braunstein, Phys. Rev. A **61**, 010302 (R) (1999).
[7] X. Jia, X. Su, Q. Pan, J. Gao, C. Xie, and K. Peng, Phys. Rev. Lett. **93**, 250503 (2004).
[8] N. Takei, H. Yonezawa, T. Aoki, and A. Furusawa, Phys. Rev. Lett. **94**, 220502 (2005).
[9] S. Bose, V. Vedral, and P. L. Knight, Phys. Rev. A **57**, 822 (1998).
[10] E. Knill, R. Laflamme, and G. J. Milburn, Nature (London) **409**, 46 (2001).
[11] H.-J. Briegel, W. Dür, J. I. Cirac, and P. Zoller, Phys. Rev. Lett. **81**, 5932 (1998).
[12] L.-M. Duan, M. D. Lukin, J. I. Cirac, and P. Zoller, Nature (London) **414**, 413 (2001).
[13] C. H. Bennett, G. Brassard, C. Crépeau, R. Jozsa, A. Peres, and W. K. Wootters, Phys. Rev. Lett. **70**, 1895 (1993).
[14] S. L. Braunstein and S. Pirandola, Phys. Rev. Lett. **108**, 130502 (2012).
[15] C. Weedbrook, S. Pirandola, R. Garcia-Patron, N. J. Cerf, T. C. Ralph, J. H. Shapiro, and S. Lloyd, Rev. Mod. Phys. **84**, 621 (2012).
[16] S. L. Braunstein and P. van Loock, Rev. Mod. Phys. **77**, 513 (2005).
[17] P. van Loock, Fortschr. Phys. **50**, 1177 (2002).
[18] M. Ohliger, K. Kieling, and J. Eisert, Phys. Rev. A **82**, 042336 (2010).
[19] J. Hoelscher-Obermaier and P. van Loock, Phys. Rev. A **83**, 012319 (2011).
[20] H. Takahashi, J. S. Neergaard-Nielsen, M. Takeuchi1, M. Takeoka, K. Hayasaka, A. Furusawa, and M. Sasaki, Nat. Photonics **4**, 178 (2010).
[21] G. Y. Xiang, T. C. Ralph, A. P. Lund, N. Walk, and G. J. Pryde, Nat. Photonics **4**, 316 (2010).
[22] A. Furusawa, J. L. Sørensen, S. L. Braunstein, C. A. Fuchs, H. J. Kimble, and E. S. Polzik, Science **282**, 706 (1998).

[23] S. Takeda, T. Mizuta, M. Fuwa, P. van Loock, and A. Furusawa, Nature (London) **500**, 315 (2013).
[24] R. E. S. Polkinghorne and T. C. Ralph, Phys. Rev. Lett. **83**, 2095 (1999).
[25] S. Takeda, T. Mizuta, M. Fuwa, H. Yonezawa, P. van Loock, and A. Furusawa, Phys. Rev. A **88**, 042327 (2013).
[26] A. Peres, Phys. Rev. Lett. **77**, 1413 (1996).
[27] E. Lombardi, F. Sciarrino, S. Popescu, and F. De Martini, Phys. Rev. Lett. **88**, 070402 (2002).
[28] D. Salart *et al.*, Phys. Rev. Lett. **104**, 180504 (2010).
[29] S. Takeda, T. Mizuta, M. Fuwa, J. Yoshikawa, H. Yonezawa, and A. Furusawa, Phys. Rev. A **87**, 043803 (2013).
[30] S. A. Babichev, J. Appel, and A. I. Lvovsky, Phys. Rev. Lett. **92**, 193601 (2004).
[31] A. I. Lvovsky, J. Opt. B **6**, S556 (2004).
[32] The experimental squeezed and antisqueezed quadrature variance is equivalent to $[(1-l)e^{\pm 2r}+l]/2$ ($\hbar=1$), where the estimated loss l ranges from 0.20 to 0.24. In the case of $l=0.22$, $r=0.71$ gives -3.9 dB of squeezing and 5.4 dB of antisqueezing, while $r=1.01$ gives -4.9 dB of squeezing and 7.9 dB of antisqueezing.
[33] G. Vidal and R. F. Werner, Phys. Rev. A **65**, 032314 (2002).
[34] M. B. Plenio, Phys. Rev. Lett. **95**, 090503 (2005).
[35] J. Eisert, Ph.D. thesis, University of Potsdam, 2001 [arXiv:quant-ph/0610253].
[36] See Supplemental Material at http://link.aps.org/supplemental/10.1103/PhysRevLett.114.100501 for additional data and details about the purification protocol.
[37] J. F. Clauser, M. A. Horne, A. Shimony, and R. A. Holt, Phys. Rev. Lett. **23**, 880 (1969).
[38] S. Massar and S. Popescu, Phys. Rev. Lett. **74**, 1259 (1995).
[39] J. Yoshikawa, K. Makino, S. Kurata, P. van Loock, and A. Furusawa, Phys. Rev. X **3**, 041028 (2013).